# SUPPLEMENTARY INFORMATION

## Theoretical Maximum Efficiency of Solar Energy Conversion in Plasmonic Metal-Semiconductor Heterojunctions

Scott K. Cushing,[a,b] Alan D. Bristow[a] and Nianqiang Wu*[b]

[a]Department of Physics and Astronomy, West Virginia University, Morgantown, West Virginia, 26506-6315, USA.

[b]Department of Mechanical and Aerospace Engineering, West Virginia University, Morgantown, West Virginia, 26506-6106, USA.
*nick.wu@mail.wvu.edu

## I. DENSITY MATRIX MODEL

### A. Extending Density Matrix to Semiconductor

In order to calculate the plasmonic enhancement the density matrix was solved using the quantum master equation as outlined in Reference S1. The treatment included the recombination time $T_1$ and the dephasing time $\frac{1}{T_2} = \frac{1}{2T_1} + \frac{1}{T_2^*}$. For the dephasing time, the factor of two times $T_1$ ensures the correct decay rate of the population and $T_2^*$ is pure dephasing, see Ref. S2. Following the formalism of Reference S1, the single particle correlations are solved in terms of spin operators in the time domain using a numerical procedure, or in the steady state by solving the resultant linear system of equations. The relevant quantities for calculation of the enhancement to solar energy conversion is then the excited state population $<\frac{1}{2} + S_i^z>$ of the plasmon and the semiconductor, as well as the polarization of the plasmon $<S_i^+ S_i^->$ which is proportional to the scattered field intensity.

The formalism of Reference S1 is for a single plasmon and semiconductor interband dipole. To replicate a semiconductor's absorption, a range of excited state populations at frequencies covering the full solar spectrum was first calculated, and then the excited state population at each frequency was multiplied by the joint density of states (JDOS) after the manner of Ref. S3. The JDOS was taken as

$$JDOS\,(\hbar\omega) = A * \Theta(\hbar\omega - E_g) \tag{S1}$$

Where $\hbar\omega$ is energy, $\Theta(x)$ is the Heaviside function, $E_g$ is the band gap, and the scaling factor $A = 30$ taken to make the plasmon and semiconductor absorption close at 3 fs plasmon dephasing, similar to the core-shell nanoparticles often used in plasmonics. The absorption tail of the Lorentzians which represent individual interband transitions in the semiconductor naturally creates an Urbach-like tail, Figure S2, modeling single-semiconductor absorption profiles common in literature. However, a 0.2 fs$^{-1}$ cut-off is necessary for each individual interband transition to avoid excessive absorption beyond the semiconductor band edge. These parameters can be modified as needed depending on the desired semiconductor absorption profile.

### B. Calculating Enhancement from Plasmon

The plasmonic enhancement was calculated from the density matrix results. First the populations and polarization of the semiconductor and plasmon were output for a frequency range covering the AM1.5G spectrum, Ref. S4, with the incident power given by the AM1.5G spectrum. At each frequency or energy to be tested the populations and polarizations were solved with and without dipole-dipole coupling in order to calculate the relative enhancements.

*Resonant Energy Transfer*- The excited state population created by resonant energy transfer was taken as the excited state population of the semiconductor with dipole-dipole coupling to the plasmon. This was converted into an effective absorption by dividing the excited state population versus frequency by the incident power, scaled

by a factor that makes the semiconductor without coupling have a peak absorption of 50%. In equation form this reads

$$\alpha_{PIRET}(\hbar\omega) = B * \frac{< \frac{1}{2} + S_{semi+plasm}^{\ z} >}{N_{AM1.5G}}$$

(S2)

where $B = -\ln(0.5)/max(< \frac{1}{2} + S_{semi}^{\ z} > /N_{AM1.5G})$ is the calibration factor which makes

$$Abs_{semi} = 1 - \exp\left(-\alpha_{semi}\right) = 50\%$$

(S3)

at the maximum of the semiconductor's absorption. The effective absorption of the plasmon is then

$$Abs_{PIRET}(\hbar\omega) = 1 - \exp(-\alpha_{PIRET}(\hbar\omega))$$

(S4)

with $S_{semi+plasm}^{\ z}$ corresponding to the spin operator for the semiconductor coupled to the plasmon, $S_{semi}^{\ z}$ corresponding to the spin operator for the semiconductor without coupling, and $N_{AM1.5G}$ the energy dependent photon density from the AM1.5G spectrum. The 50% absorption at peak of the semiconductor corresponds to a specific absorption cross section times a thickness.

*Hot electrons*- The excited state population created by hot electrons was taken as the plasmon excited state population with dipole-dipole coupling times a transfer rate, plus the excited state population of the semiconductor without dipole-dipole coupling or scattering. Again, this was converted into an effective absorption by dividing the combined population versus frequency by the incident power, scaled by a factor that made the semiconductor without coupling have a peak absorption of 50%. In equation form this reads

$$\alpha_{HE}(\hbar\omega) = B * \frac{< \frac{1}{2} + S_{plasm+semi}^{\ z} >* \Gamma_{HE} + < \frac{1}{2} + S_{semi}^{\ z} >}{N_{AM1.5G}}$$

(S5)

giving

$$Abs_{HE}(\hbar\omega) = 1 - \exp(-\alpha_{HE}(\hbar\omega))$$

(S6)

with $S_{plasm+semi}^{\ z}$ corresponding to the spin operator for the plasmon coupled to the semiconductor, $\Gamma_{HE}$ corresponding to hot electron transfer rate taken as 10% from Ref. S5, and $S_{semi}^{\ z}$ corresponding to the spin operator for the semiconductor without coupling.

*Scattering*- The enhancement in semiconductor absorption by scattering was calculated by outputting the polarization of the plasmon when coupled by dipole-dipole interactions to the semiconductor, then scaling the amplitude of the polarization. The scaling factor, $C = 1500 * B$, was chosen so that at 8-10 fs plasmon dephasing the

semiconductor without dipole-dipole coupling would absorb almost all light scattered by the plasmon, representing multiple reflections or a light trapping efficiency of 100% at the plasmon's scattering peak. In equation form this reads

$$\alpha_{scatt}(\hbar\omega) = C * \frac{< S_{plasm+semi}^{+} S_{plasm+semi}^{-} >}{N_{AM1.5G}}$$ (S7)

where $< S_{plasm+semi}^{+} S_{plasm+semi}^{-} >$ is the polarization of the plasmon coupled to the semiconductor. Equation S7 therefore corresponds to some given number of reflections, of which can allow the semiconductor to re-absorb light not converted on the first pass, as given by

$$Abs_{Scatt}(\hbar\omega) = \left[1 - \exp\left(-\alpha_{semi}(\hbar\omega)\right)\right] + \left[\left(1 - \left(1 - \exp\left(-\alpha_{semi}(\hbar\omega)\right)\right)\right) * \left(1 - \exp\left(-\alpha_{scatt}(\hbar\omega) * \alpha_{semi}(\hbar\omega)\right)\right)\right]$$ (S8)

It should be noted $C = 1000$ was used in Fig. S4 for 100% light trapping at 15 fs.


Through this method, an effective absorption was created that considered the enhancement of each mechanism independently on the semiconductor but through a single plasmon source. As noted in the manuscript, the losses from hot electrons were neglected because interface dampening can have a much larger effect, Ref S6.

For the combined calculation in Figure 5 the same approach was taken, but now combining the hot electron population to the semiconductor absorption with dipole-dipole coupling, and taking this as the initial absorption in Equation S8. The scattering then causes multiple reflections

$$Abs_{overall}(\hbar\omega)$$
$$= \left[1 - \exp\left(-\left(\alpha_{PIRET}(\hbar\omega) + \alpha_{HE-only}(\hbar\omega)\right)\right)\right] + \left[\left(1 - \left(1 - \exp\left(-\left(\alpha_{PIRET}(\hbar\omega) + \alpha_{HE-only}(\hbar\omega)\right)\right)\right.\right.\right.$$ (S9)

where $$\alpha_{HE-only}(\hbar\omega) = B * \frac{< \frac{1}{2} + S_{plasm+semi}^{z} >* \Gamma_{HE}}{N_{AM1.5G}}$$ to avoid double counting the semiconductor from Equation S5.

## C. Calculating Solar Energy Conversion

Once the effective absorption of the plasmon was calculated, this was turned into a conversion efficiency by first determining the number of photons absorbed

$$N_{photons} = \int d(\hbar\omega)\, Abs_i(\hbar\omega) * N_{AM1.5G}(\hbar\omega)$$ (S10)

where $Abs_i(\hbar\omega)$ is the effective absorption to be used from the above enhancement mechanisms and $N_{AM1.5G}(\hbar\omega)$ is again the photon density per energy in the AM1.5G spectrum. The loss due to carrier thermalization was then included as

$$R_0 = \frac{2\pi}{c^2 h^3} * \int d(\hbar\omega) \, Abs_i(\hbar\omega) * \frac{(\hbar\omega)^2}{\exp\left(\frac{\hbar\omega}{K_b T}\right) - 1}$$

(S11)

where $c$ is the speed of light, $h$ is Plank's constant, $K_b$ Boltzmann's constant, and $T$ the temperature of the solar cell. For heating losses the effective absorption was used, except in the case of hot electrons where the absorbed carriers were offset $E_g/2$ from the plasmon frequency when added to the semiconductor to represent an intrinsic Schottky barrier.

For photovoltaics the current density and maximum efficiency were determined by

$$J(V) = q * \left( N_{photons} - R_0 * \exp\left(\frac{V}{K_b T}\right) \right)$$

(S12)

and

$$Eff_{PV} = max(V * J(V))/P_{AM1.5Gtotal}$$

(S13)

where $P_{AM1.5Gtotal}$ is the total power in the AM1.5G spectrum. For solar to chemical conversion this is modified to

$$Eff_{PEC} = J(0) * (E_g - 0.8 - 0.5)/P_{AM1.5Gtotal}$$

(S14)

where the 0.8 eV loss is intrinsic losses including thermodynamics effects as justified in Reference S7, and the 0.5 eV factor takes into account the absorption tail.

**D. Overall Calculation Flow and Input Parameters**

The overall calculation flow is represented in Figure S3 and was repeated for a range of plasmon energies, semiconductor band gaps, and plasmon dephasings. The resulting data set was then used to find the maximum conversion efficiencies as reported in the main text.

The input parameters were unless otherwise noted: $\mu_{plasmon} = 1.5e-27 \ Cm$ estimated from Ref. S8 and $T_{1plasm} = 1 \ ps$ estimated from average electron-phonon relaxation times in Ref. S9; $\mu_{semiconductor} = 1e-28 \ Cm$ estimated from Ref. S10 and also as roughly charge times the lattice constant, with $T_{1semi} = 1 \ ps$ estimated from Ref. S11 and $T_2^* = 10 \ fs$ estimated from Ref. S13. The input field strength varied as the AM1.5G spectrum. The close distance of the plasmon and semiconductor allowed the cooperative emission term to be neglected as justified in Ref. S1. The dipole-dipole coupling was taken as $V = 0.001$ fs-1, which given the dipole moments used, corresponds to an orientation averaged separation of ~20 nm between the plasmon and semiconductor centers. Given that most plasmonic nanoparticles with ~10-15 nm in radius have a few fs dephasing time, and that the size effects are being neglected in this approximation, this corresponds to a plasmon to semiconductor surface distance of ~5-10 nm.

**II. FIGURES**
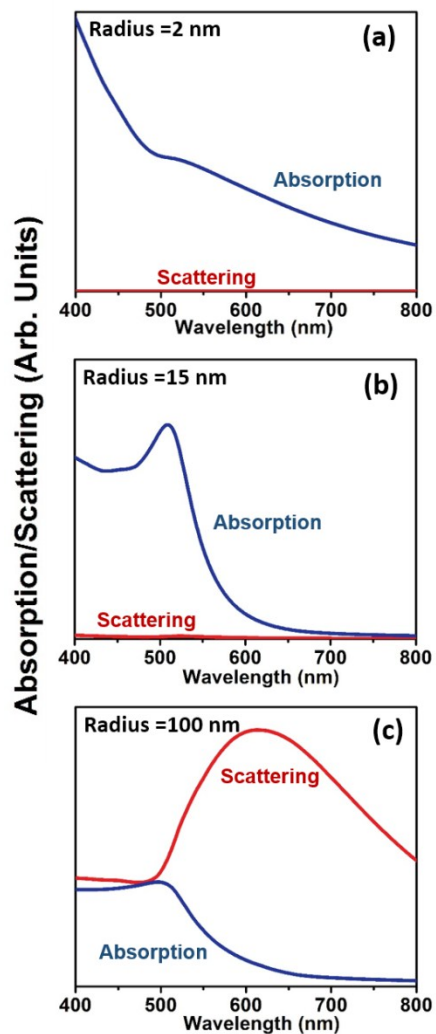


**Fig. S1** Evolution of absorption and scattering cross sections with size of a Au nanoparticle. For a 2 nm Au nanoparticle, the plasmon quickly dephases, leading to a weak resonant absorption. As the size is increased to 15 nm, the resonant absorption increases, however the scattering efficiency is still low. For a 100 nm spherical gold nanoparticle, the scattering dominates the optical response. The optical properties were calculated using Mie theory, see Reference S12. The 2 nm Au nanoparticle used a surface-damped and size-dependent dielectric constant, see Reference S13, and a proportionality constant of seven to represent surface dampening.
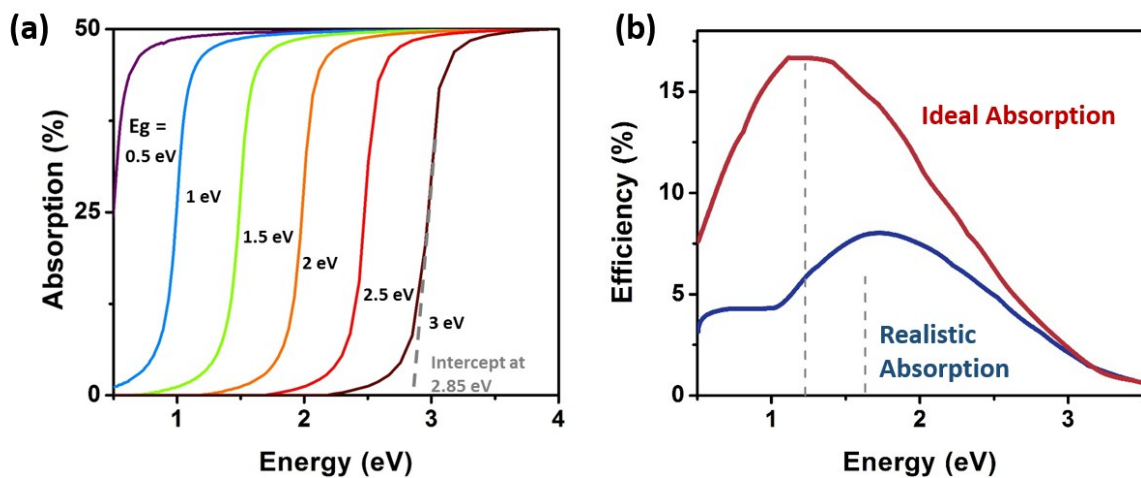
**Fig. S2** Absorption calculated using the density matrix model of the semiconductor for several band gaps. (a) The absorption is calculated as the percent of incident light which created an excited state population in the steady-state limit. Note that the band gap is more representative of the initial rise of the absorption than the intersection with the axis due to the Urbach tail modeled, shifting the band gap ~0.15 eV from the intercept with the axis. (b) Since an absorption profile is used, and not an assumed 100% absorption at the band gap, the maximum efficiency calculations for the semiconductor alone are offset in energy. The ideal absorption is calculated using a Heaviside function at the band gap value scaled to 50% absorption. The realistic absorption is that in (a).
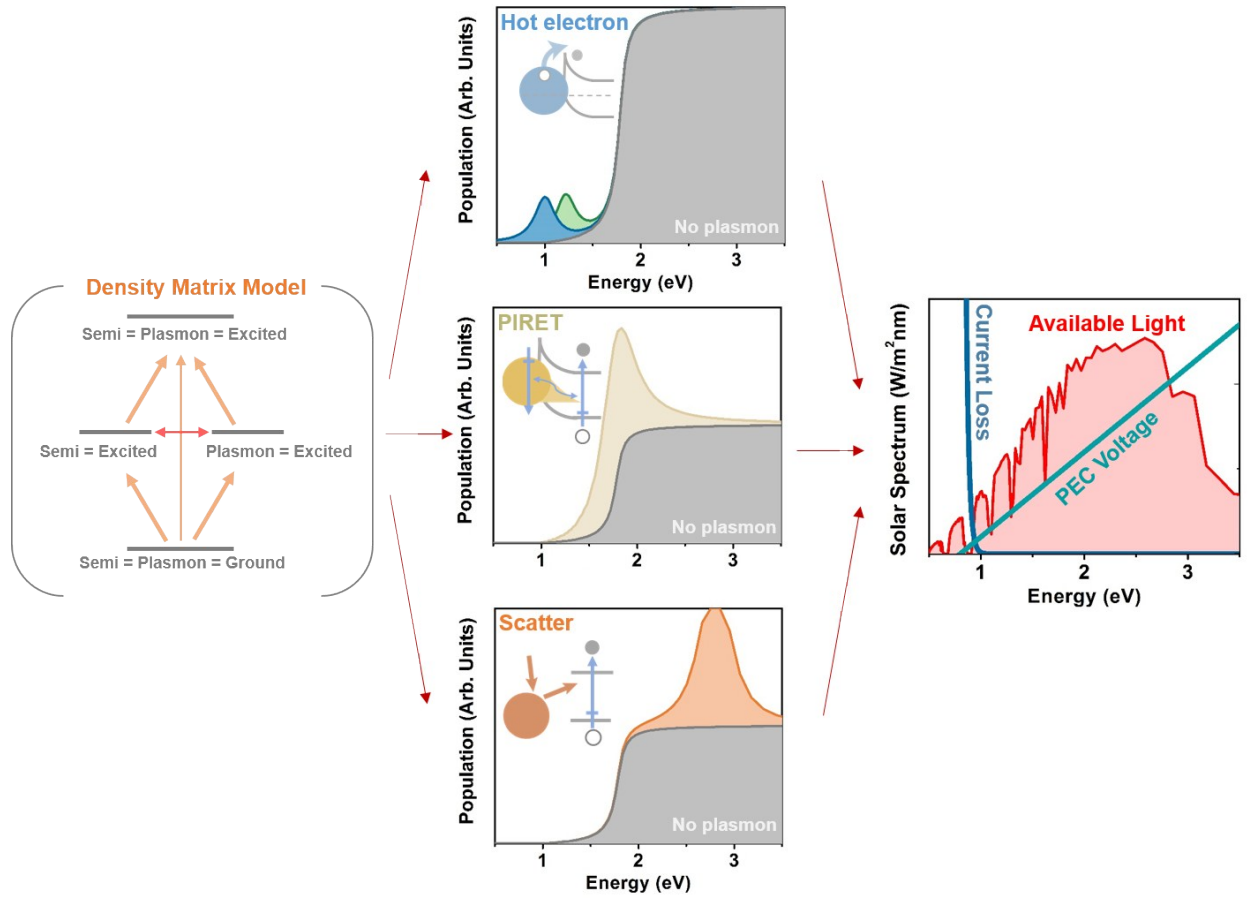
**Fig. S3** Schematic of maximum efficiency calculations using the density matrix. The coupled density matrix representing the plasmon and semiconductor is first solved in the steady state, giving the excited state populations and polarizations of the plasmon and semiconductor. The enhancement in semiconductor population by dipole-dipole coupling is translated into an effective absorption to describe PIRET. The plasmon's population is multiplied by a transfer rate and added to the semiconductor population to represent hot electron transfer. Carriers are added to the semiconductor at $E_g/2 + E_{plasmon}$. The effective absorption and thermalization from hot electron transfer are then calculated from these properties. The scattering to absorption efficiency is calculated, and then the probability for the semiconductor to re-absorb light scattered with this efficiency is found. The three effective absorptions are integrated over the solar spectrum to find the number of photons absorbed, with thermalization losses subtracted at the corresponding maximum power point. For PEC the short circuit current and band edge voltage minus 0.8 eV in losses is used, along with an offset of 0.5 eV to account for the absorption tail in Fig. S2.
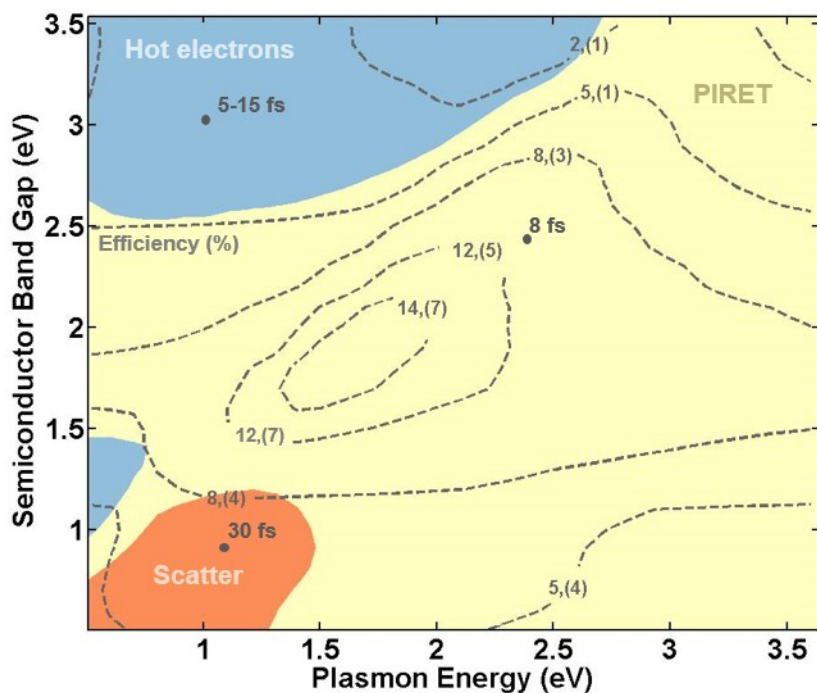
**Fig. S4** Maximum efficiency for solar energy conversion of an AM1.5G spectrum through photovoltaics. The plasmonic enhancement mechanism responsible for the maximum conversion efficiency at a plasmon-semiconductor energy combination is shown, similar to Fig. 4a, however the efficiency of the scattering has been changed from 100% light trapping at 8-10 fs to 100% light trapping at 15 fs. This highlights the similar enhancement percentage by PIRET and scattering in the above band gap region. The maximum efficiency is labeled on each contour, along with the value from the semiconductor alone at that point in parenthesis. The dephasing at several points across the graph which led to the maximum enhancement is also shown.

## III. REFERENCES

S1. G. V. Varada and G. S. Agarwal, *Phys. Rev. A*, 1992, **45**, 6721.

S2. L. Mandel and E. Wolf, in *Optical Coherence and Quantum Optics,* Cambridge University Press, New York, 1995.

S3. P. C. Becker, H. L. Fragnito, CH Brito Cruz, R. L. Fork, J. E. Cunningham, J. E. Henry and C. V. Shank, *Phys. Rev. Lett.*, 1988, **61**, 1647.

S4. http://rredc.nrel.gov/solar/spectra/am1.5/

S5. A. J. Leenheer, P. Narang, N. S. Lewis and H. A. Atwater, *J. Appl. Phys.,* 2014, **115***, 134301.

S6. J. Li, S. K. Cushing, F. Meng, T. R. Senty, A. D. Bristow, N. Q. Wu, Nature Photonics, 2015, 10.1038/NPHOTON.2015.142.

S7. J. Bolton, S. Strickler and J. Connolly, *Nature*, 1985, **316**, 495.

S8. X. Liu, M. Atwater, J. Wang and Q. Huo, *Colloids Surf. B*, 2007, **58**, 3.

S9. S. Link and M. A. El-Sayed, *J. Phys. Chem. B*, 1999, **103**, 8410.

S10. E. Rosencher, in *Optoelectronics*, Cambridge University Press, New York, 2002.

S11. J. Shah, in *Ultrafast Spectroscopy of Semiconductors and Semiconductor Nanostructures*, Springer, New York, 1999.

S12. O. Peña-Rodríguez, P. P. G. Pérez, and U.a Pal, *Int. J. Spectrosc.* 2011, **2011,** 583743.

S13. L. B. Scaffardi, N. Pellegri, O. de Sanctis and J. O. Tocho, *Nanotechnology*, 2005, **16,** 158.